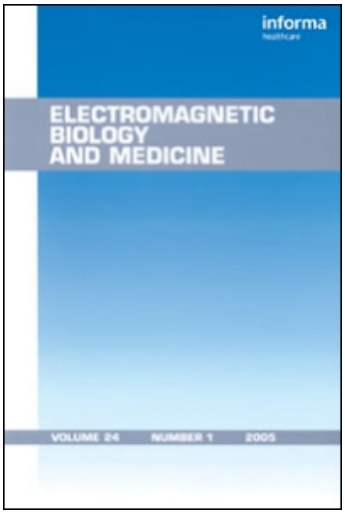

Electromagnetic Biology and Medicine
Publication details, including instructions for authors and subscription information:
http://www.informaworld.com/smpp/title~content=t713597249

APOPTOSIS OF EHRLICH MOUSE ASCITES CELLS INDUCED BY LONG-TERM EXPOSURE OF WEAK ELECTROMAGNETIC FIELDS IN VIVO

Hong-Li Jiao [a]; Yan Wang [a]; Jiin-Ju Chang [a]
[a] Chinese Academy of Sciences, Institute of Biophysics, Chaoyang District, Beijing, People's Republic of China

Online publication date: 30 November 2001

To cite this Article Jiao, Hong-Li, Wang, Yan and Chang, Jiin-Ju(2001) 'APOPTOSIS OF EHRLICH MOUSE ASCITES CELLS INDUCED BY LONG-TERM EXPOSURE OF WEAK ELECTROMAGNETIC FIELDS IN VIVO', Electromagnetic Biology and Medicine, 20: 3, 299 — 311
To link to this Article: DOI: 10.1081/JBC-100108571
URL: http://dx.doi.org/10.1081/JBC-100108571

ELECTRO- AND MAGNETOBIOLOGY, 20(3), 299–311 (2001)

APOPTOSIS OF EHRLICH MOUSE ASCITES CELLS INDUCED BY LONG-TERM EXPOSURE OF WEAK ELECTROMAGNETIC FIELDS IN VIVO

Hong-Li Jiao, Yan Wang, and Jiin-Ju Chang*

Institute of Biophysics, Chinese Academy of Sciences, 15 Dantun Road, Chaoyang District, Beijing 100101, People's Republic of China

ABSTRACT

To study the possibility of apoptosis of tumor cells induced by weak electromagnetic fields (EMFs) in vivo, mice were inoculated with Ehrlich ascites cells and exposed to a long-term electromagnetic field (1 mT, 700 KHz). During the treatment, growth curves of mice were measured and compared between exposed and sham-exposed mice. The results show that the growth curves of healthy controls agree well with the ideal curve of logistic growth, but the growth curves of cancer mice deviate from the ideal curve. There is no difference in growth curves between exposed, and sham-exposed healthy mice, and they both agree with the ideal curve. However, a notable difference in growth curves between exposed and sham-exposed cancer mice was obtained. Moreover, the curves of sham-exposed mice deviate even more than those of the exposed mice; in other words, the growth curves of Ehrlich ascites mice deviate from the ideal curve of healthy mice but are shifted toward it by the EMF treatments. After the treatment, apoptosis of Ehrlich ascites cells from inoculated mice was analyzed by several methods, including flow cytometry, fluorescence microscopy, and DNA gel electrophoresis. Statistical analysis from flow cytometry shows that the apoptotic ratio of cells from exposed Ehrlich ascites mice was significantly higher than that from sham-exposed treated mice. Microscopic observation of Ehrlich ascites cells stained with

* Corresponding author. Fax: 0086-10-64888428; E-mail: changjj@sun5.ibp.ac.cn

acridine orange (AO) and propidium iodide (PI) showed typical apoptotic changes in exposed animals whose cell nuclei were highly condensed or fragmented and uniformly stained green by the AO, whereas cell nuclei from sham-exposed mice were stained green and showed a fine reticular pattern. Agarose gel electrophoresis of DNA from exposed mice showed that the chromatin DNA exhibited ladders, a characteristic feature of internucleosomal degradation of DNA by EMF treatments. For interactions between external electromagnetic fields and DNA, the mechanism of apoptosis of tumor cells induced by weak EMFs is discussed.

Key Words: Apoptosis; Ehrlich ascites cells; Long-term exposure; Weak electromagnetic fields (EMFs)

INTRODUCTION

Apoptosis, or programmed cell death, plays a major role during development, homeostasis, and in many human diseases, including cancer. The ''decision'' of cells to undergo apoptosis can be influenced by a wide variety of stimuli, and is regulated by many different signals originating from both extracellular and intracellular environments (1).

Tumors develop not only from abnormal cell proliferation and inhibition of differentiation, but also from reduced cell death due to inhibition of apoptosis (2). Promoting apoptosis of tumor cells is a new strategy for cancer treatment.

Recently, apoptosis in various cell types, induced by electromagnetic fields (EMFs), has been reported from several laboratories (3–5). However, up to now, research reports concerning apoptosis of tumor cells induced by EMFs in vivo have not appeared. To address the possibility of apoptosis of tumor cells induced by exposure of weak EMFs to animals, Ehrlich ascites mice were exposed to a weak EMF at 700 KHz and 1 mT, and the apoptosis of the cancer cells from exposed and sham-exposed mice was analyzed by flow cytometry, fluorescence microscopic assay, and DNA gel electrophoresis. According to our scanning measurements, the EMF absorbance is the highest at this frequency for many biological materials, such as chicken embryos and mice. In this article, the preliminary experimental results are presented.

MATERIALS AND METHODS

Animals and EMF Treatment

Mice [male, 20 ± 2 g, *Mus musculus* (km)] used in this study were purchased from the Animal Center, Institute of Genetics, Chinese Academy of Sciences. The mice were given food and water *ad libitum*. To induce Ehrlich ascites in mice, each was inoculated with 0.3 ml of the cells at a concentration of 2×10^7 cells/ml. The experimental exposure condition is shown in Figure 1. Exposed mice

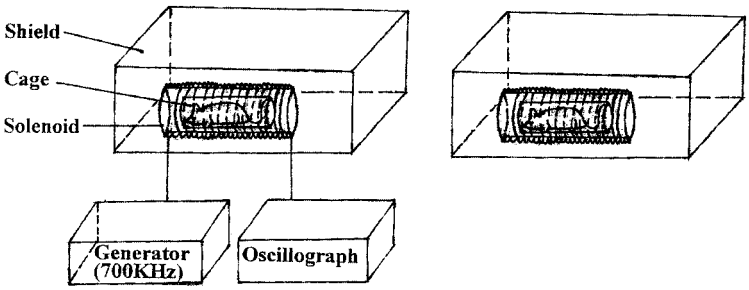

Figure 1. The experimental exposure condition.

were placed in a solenoid connected to a generator which produced a 700 KHz, 1 mT alternating sinusoidal magnetic field.

The mouse cage in the solenoid was specially made, and was narrow enough to limit the movement of the exposed mouse. The long axis of the mouse was parallel with the magnetic force line of the EMF and parallel to the Earth's field. Sham-exposed mice were handled under the same conditions but without connection with the generator, and served as the controls for the treatments.

In this coil, the specific absorption rate (SAR) of exposed mice is about 0.3–0.5 mW/g. The room temperature was controlled at 25°C.

Thermal effect was monitored by measuring the changes of temperature inside of the solenoid with a thermometer. No visible temperature increase was observed during the exposures. Healthy mice were taken as the controls for inoculated mice. In this study, mice were treated in three groups (Table 1). The course of exposure was 10 days for group 2 and 8 days for group 3. The treated mice were exposed 6 hr each day. During the treatments, the weight of each mouse was measured every day and growth curves were made according to statistical means of the measurements.

Flow Cytometric Analysis of Apoptosis

Ehrlich ascites cells were drained from the abdomens of exposed and sham-exposed mice with a syringe. After cells were sterilized with 75% ethanol, centri-

Table 1. The Characteristics of the Groups

Group No.	Number of Unexposed	Number of Sham Exposed	Number of Exposed
1	9 Healthy mice	9 Healthy mice	9 Healthy mice
2	8 Healthy mice	8 Inoculated mice	8 Inoculated mice
3	9 Healthy mice	9 Inoculated mice	9 Inoculated mice

Mice in group 2 were exposed right after inoculation, in group 3 they were exposed on the seventh day after inoculation.

fuged, and washed in phosphate-buffered saline (PBS), they were then resuspended at 10^6 cells/ml with PBS. Propidium iodide (PI) was added in a final concentration of 5 μg/ml. The cells were stained for 30 min, and then directly analyzed by flow cytometry (FACScan, Becton Dickinson, San Jose, CA). The program of CellFIT Cell-Cycle Analysis version 2.01.02 was used to analyze cell cycle phase. The apoptotic ratio was analyzed by the program of LySYS II version 1.1.

Fluorescence Microscopic Assay of Apoptotic Nuclei

Cells from exposed and sham-exposed animals were collected and stained with a dye mixture of 10 μg/ml acridine orange (AO) and 10 μg/ml PI, then examined under a Nikon fluorescence microscope to determine which cells were undergoing nuclear changes characteristic of apoptosis. AO (a fluorescent DNA-binding dye) intercalates into DNA, making it appear green, and also binds to RNA, staining it red–orange. PI is taken up only by nuclei of nonviable cells, and its fluorescence overwhelms that of the AO, making the chromatin of dead or lysed cells appear red (6).

Agarose Gel Electrophoresis of DNA

A total of 10^6 cells from each treated or sham-treated mouse were harvested by centrifugation at 4000 $\times$ g for 4 min, the supernatant was removed, and the cells were resuspended in 500 μl of lysis buffer (100 mM Tris, 5 mM ethylenediaminetetraacetic acid [EDTA], 200 mM NaCl, 0.2% sodium dodecyl sulfate [SDS], pH 8.5). Twenty microliters of proteinase K (10 mg/ml) was added and the lysed cells were incubated at 50°C for 2 hr and cooled to 0°C. An equal amount of cold ethanol (at −20°C) then was added to precipitate DNA, which was collected by centrifugation (12,000 $\times$ g, 30 min), dried in air, and dissolved in 50 μl TE buffer (10 mM Tris, 1 mM EDTA at pH 8.0). Each DNA preparation was mixed with 2 μl RNase (10 mg/ml) and 6 μl loading buffer (0.25% bromophenol blue, 0.25% xylene cyanol, and 30% glycerol dissolved in deionized H_2O) and incubated for 15 min at 37°C. Samples were then run on a 1.6% agarose gel containing 0.5 μg/ml ethidium bromide (EB), at 2.5 V/cm for 1.5 hr. The gel was then observed under ultraviolet light and photographed.

Statistics

All data are expressed as mean ± standard error (SE). Data were processed by using a program of Statistic, Inc. Statistical significance was assessed by the Student's t-test ($p < 0.05$).

MARCEL DEKKER, INC.
270 Madison Avenue, New York, New York 10016

RESULTS

Difference in Growth Curves

Growth curves of mice are shown in Figures 1–3, where the curves of exposed, sham-exposed, and healthy control mice are shown by solid lines, broken lines, and dotted lines, respectively. According to the logistic growth model (7), the ideal curve of growth for healthy mice is illustrated by the thick dashed line.

Figure 2 shows that there is no difference in growth curves between exposed and sham-exposed healthy mice, and they both fit well with the ideal curve. From Figures 3 and 4, a notable difference in growth curves between exposed and sham-exposed cancer mice was obtained.

It is obvious that the growth curves of healthy controls fit well with the ideal curve, but the growth curves of cancer mice deviate from the ideal curve. Moreover, the curves of sham-exposed mice deviate more than those of the exposed mice. In other words, the growth curves of exposed mice are closer to the ideal curve. In Figure 4, an identical difference in growth curves between exposed and sham-exposed inoculated mice in group 3 only can be seen after day 7, when the treatments were undertaken. Comparing Figure 2 with Figure 4, the difference

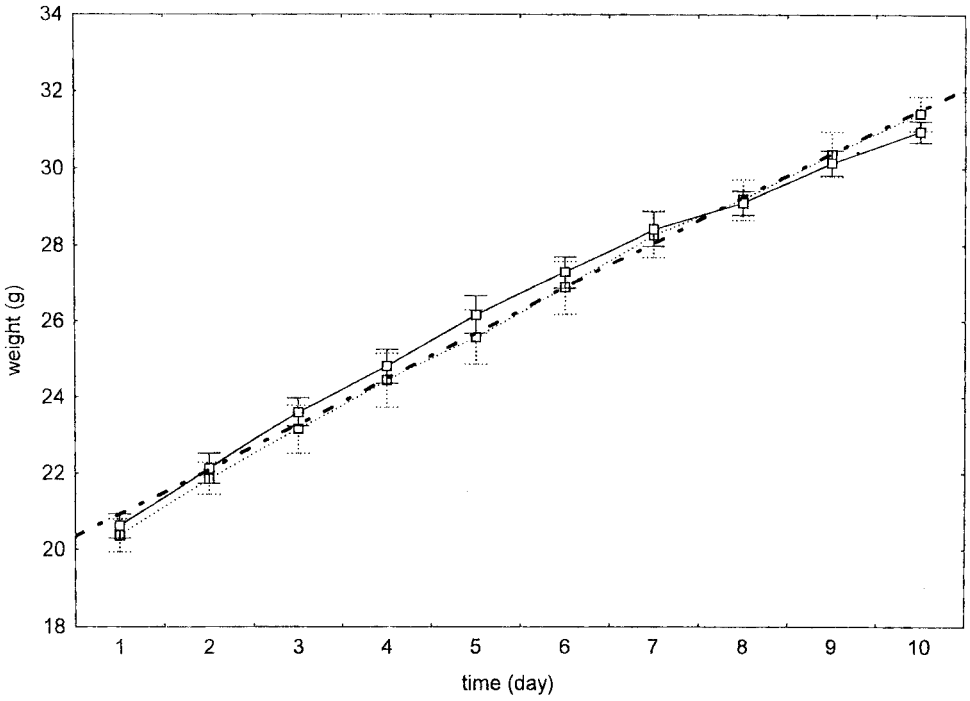

Figure 2. Growth curves of healthy mice in group 1. Each curve was constructed from statistical averages of 9 mice ($n = 9$). The solid line describes the growth curve of exposed mice; the broken line shows the growth curve for sham-exposed mice. The thick dashed line shows the ideal growth curve of unexposed healthy mice according to the logistic growth model.

MARCEL DEKKER, INC.
270 Madison Avenue, New York, New York 10016

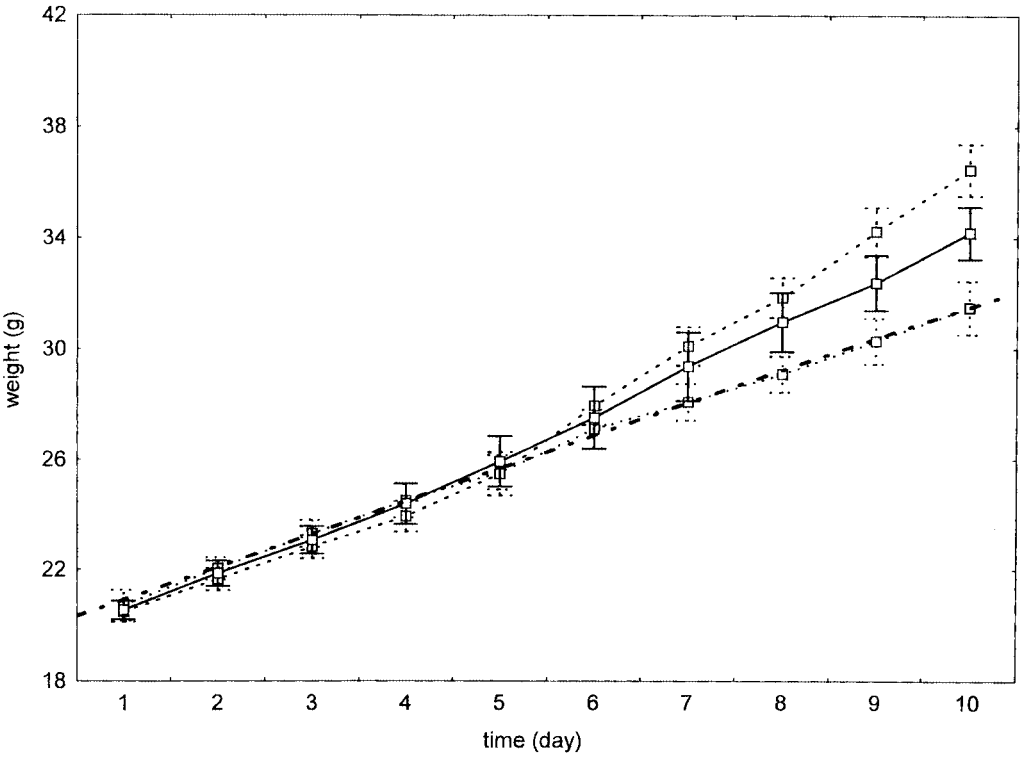

Figure 3. Growth curves of cancer mice in group 2 where EMF treatments were carried out immediately after the inoculation. Each curve was constructed from statistical means of 8 mice ($n = 8$). Growth curves of exposed, sham-exposed, and unexposed healthy mice are described by solid lines, broken lines, and dotted lines, respectively. The thick dashed line shows the ideal growth curve of healthy mice according to the logistic growth model.

in the growth curves between early exposed and sham-exposed cancer mice in group 2 is greater than between those of late-exposed and sham-exposed mice in group 3.

Changes in Cell Cycles Analyzed by Flow Cytometry

Figure 5 shows typical changes in cell cycles of Ehrlich ascites cells analyzed by flow cytometry with Cell FIT software. Figure 5(A) is a histogram of DNA content from sham-exposed mice and Figure 5(B) is from exposed mice in group 2. The percentages in G0–G1, G2–M, and S phases are 27.83, 32.06, and 40.11% in (A), and 33.03, 29.34, and 37.63% in (B), respectively. No apoptotic peak was observed in the sham-exposed control. Compared with the control, the number of cells in S–M and G2–M phase as a fraction of the total cells decreased, and the number of cells in G0–G1 phase increased in the treated animals. A distinct

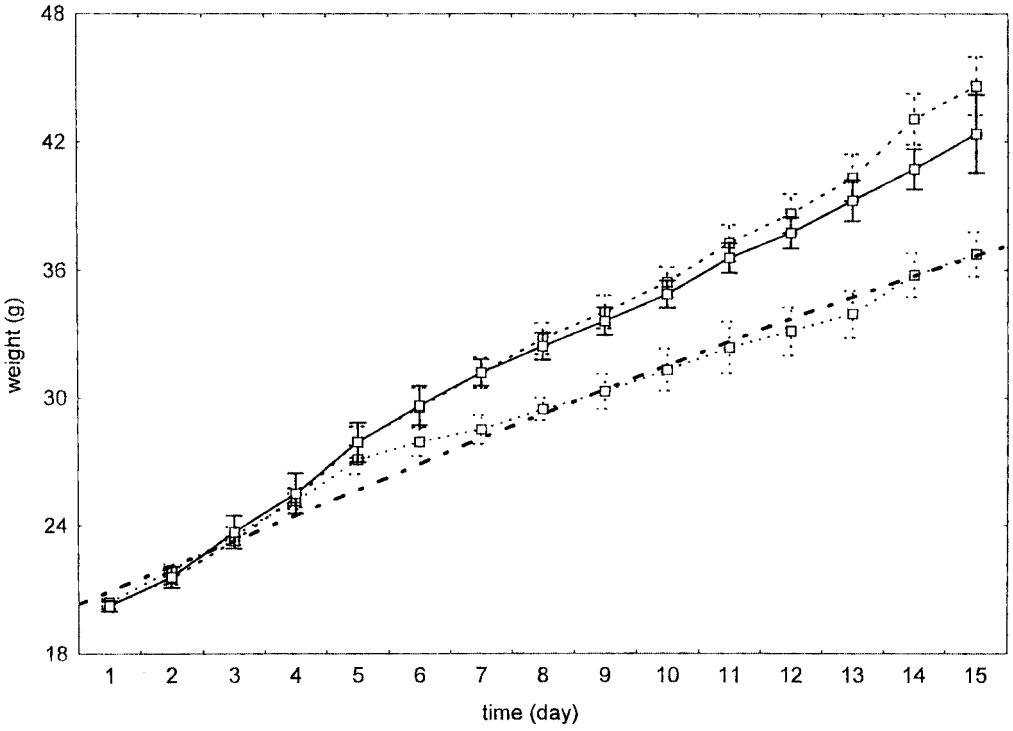

Figure 4. Growth curves of cancer mice in group 3, where EMF treatments were begun on day 7 after inoculation. Each curve was the result of statistical means of 9 mice ($n = 9$). Growth curve of exposed, sham-exposed, and unexposed healthy mice are described by solid lines, broken lines, and dotted lines, respectively. The thick dashed line shows the ideal growth curve of unexposed healthy mice according to the logistic growth model.

population of apoptotic cells in sub-G1 phase (apoptosis peak, AP) appeared. The apoptotic cells were about 9.40% of the population.

The results indicated that EMFs can promote apoptosis of Ehrlich ascites cells in vivo. The apoptosis of Ehrlich ascites cells might be associated with G1 arrest. The characteristics of the cell cycle from cancer mice in group 3 were similar to those in group 2 (data not shown).

Difference in Apoptosis Levels Analyzed by Flow Cytometry

To observe the effects of weak EMFs on apoptosis of Ehrlich ascites cells in vivo, the apoptosis ratio was analyzed by flow cytometry with LySYS II software. The statistical averages of apoptosis ratios of cells from exposed and sham-exposed cancer mice in group 2 were 5.460 ± 2.927 and 0.889 ± 0.995 ($n = 8$), respectively. The average apoptotic ratios of cells from exposed and sham-exposed animals in group 3 were 9.729 ± 1.791 and 4.131 ± 1.035, respectively

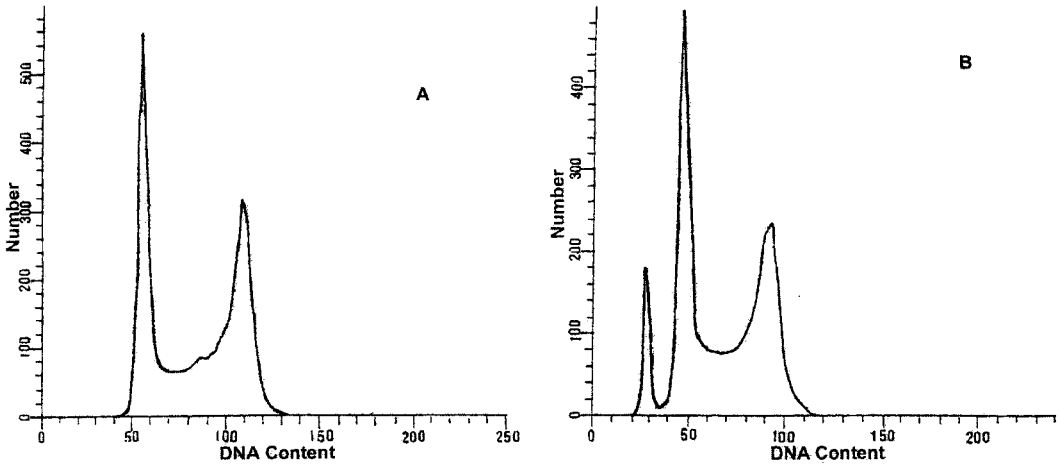

Figure 5. Typical histograms of DNA contents showing differences in cell cycle phases and apoptosis of Ehrlich ascites cells from sham-exposed controls (A) and EMF treated mice (B). A distinct population of apoptotic cells in sub-G1 phase (apoptosis peak, AP) was identified in (B). The apoptotic cells were about 9.40% of the population.

($n = 9$). Figure 6 shows that the average apoptotic ratios of cells from exposed Ehrlich ascites mice is significantly ($p < 0.05$) higher than those from sham-exposed mice, and the difference between exposed and sham-exposed mice in group 2 was greater than that in group 3.

Morphological Changes Observed by Fluorescence Microscope

Under the fluorescence microscope, we observed morphological changes of Ehrlich ascites cells stained with AO and PI from mice of group 2. As shown in Figure 7, cell nuclei from sham-exposed controls (A) were stained green and appeared as a fine reticular pattern, whereas cell nuclei from exopsed animals (B) were highly condensed or fragmented, and were uniformly stained green by the AO, demonstrating that there were typical apoptotic changes in cells from exposed animals. Cells from the mice in group 3 appeared to have similar morphological changes (data not shown).

Characteristics Assayed by Agarose Gel Electrophoresis of DNA

Figure 8 is and illustration of agarose gel electrophoresis of DNA from exposed and sham-exposed mice in group 2, showing that the chromatin DNA exhibited ladders, a characteristic feature of internucleosomal degradation of DNA by the EMF treatments. This result also demonstrated that apoptosis of cells occurred

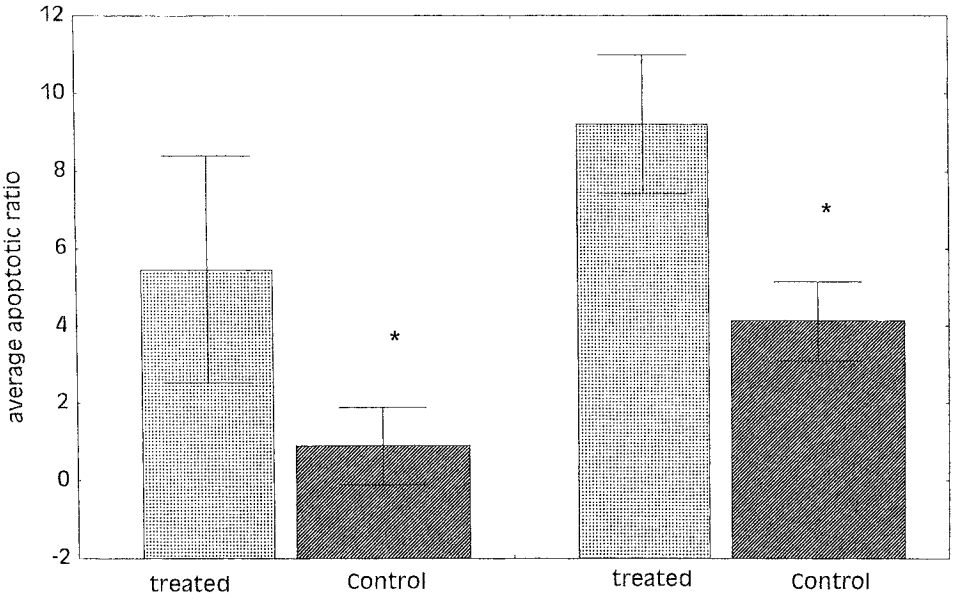

Figure 6. Statistical averages of apoptotic ratios of cells from exposed and sham-exposed mice in group 2 (left, $n = 8$) and in group 3 (right, $n = 9$) showing that the average apoptotic ratios in cells from exposed Ehrlich ascites mice were significantly higher than those from sham-exposed mice ($p < 0.05$).

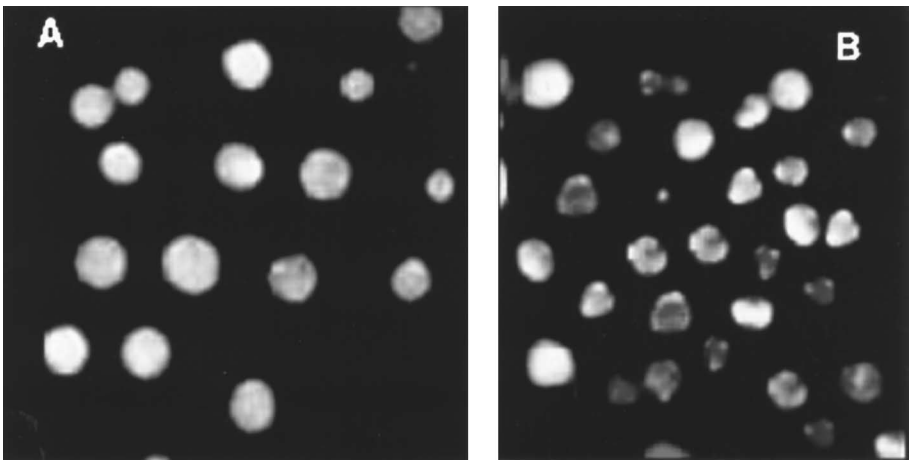

Figure 7. Fluorescence micrographs of Ehrlich ascites cells in control (A) and treated (B) mice in group 2 after cell staining with AO and PI: The cells from sham-exposed mice were stained green and appeared in a fine reticular pattern. The cells from exposed animals were highly condensed or fragmented and uniformly stained green by the AO.

MARCEL DEKKER, INC.
270 Madison Avenue, New York, New York 10016

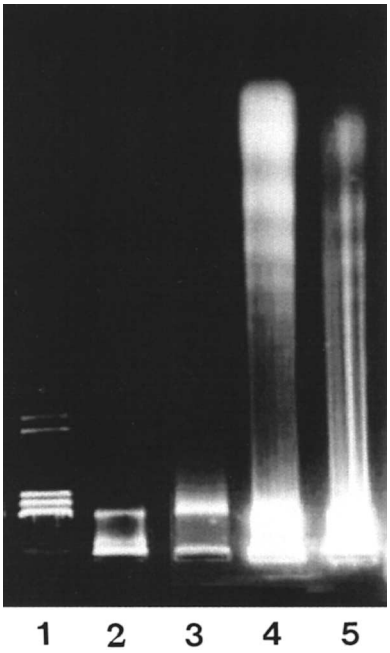

Figure 8. Agarose gel electrophoresis of DNA of the cells from exposed mice and sham-exposed mice. Lane 1-marker (Hind III /Hae III; GIBCO); lane-2,3 EMFs sham-exposed mice of Groups 2 and 3; lanes 4 and 5: and EMF-exposed mice of Groups 2 and 3. The chromatin DNA exhibited ladders, a characteristic feature of internucleosomal degradation of DNA.

after the animals were exposed to weak EMFs. Analysis of agarose gel electrophoresis of DNA from group 3 yielded similar results.

DISCUSSION

It has become generally accepted that EMFs cause various biological effects (8,9) and thus they have been used for some clinical purposes; for instance, for promoting neural regeneration and bone healing. However, whether certain EMFs can be used for cancer treatment has remained unknown until now. In the present report, we provide evidence that long-term exposure of Ehrlich ascites mice to weak EMFs promoted apoptosis of the cancer cells and inhibited the deviation of the growth curves of the cancer mice from the ideal growth curve of healthy mice. This suggests that EMFs may damage cancer cells by inducing apoptosis. This result confirmed the findings of some previous experiments. Hisamitsu et al. (3,4) found that EMFs could induce apoptosis of cultured human myelogenous leukemia cell lines HL-60 and ML-1 in vitro. Ismael et al. (5) reported that EMFs accelerated dexamethasone-induced apoptosis of mouse thymocytes in vivo. Blumenthal et al. (10) found that EMFs may initiate the apoptosis of rat tendon fibro-

MARCEL DEKKER, INC.
270 Madison Avenue, New York, New York 10016

blast (RTF) and rat bone marrow (RBM) osteoprogenitor cells in vitro and result in significant alteration in cell metabolism and cytoskeleton structure.

To determine the mechanism of induced apoptosis by EMFs, it is important to discuss the mechanism of interaction between weak EMFs and living systems; in particular, between weak EMFs and DNA. Blank (11) believed that direct interaction of EMF with DNA should be considered as a possible mechanism. Recently, an interference model has been suggested by Popp and Chang (12). According to these authors, destructive interference of incoming and reflected waves is established outside of the living cells. As a consequence, on the inside, constructive interference takes place at the same time.

The results of the interaction depend not only on EMFs, but also on the characteristics of the biological matter. Therefore, it may happen that under certain conditions, tumor cells are more sensitive to EMFs than are normal cells, since their DNAs are in different excited states. The synergistic effects of EMF exposure and X-ray or chemotherapy in vitro can be easily understood from this point. Cadossi et al. (13,14) pointed out that mice irradiated with X-ray and then exposed to pulsing EMF (PEMF) suffered more rapid decline in white blood cells in peripheral blood than mice that were only irradiated, and that the growth of bone marrow and spleen cells was inhibited more strongly. They also found that mice injected with cyclophosphamide (CY) and then exposed to PEMF showed increase in the damage induced in mice by the CY. In addition, Flipo et al. (15) demonstrated the correlation between apoptosis of thymic cells and lymphocytes with Ca^{2+} influx into the cells. There were also numerous other hypotheses dealing with the mechanism of interactions between EMFs and living systems (16–21).

Although the detailed mechanism of apoptosis induced by weak EMFs remains to be elucidated, these experimental results show that EMFs may have a valuable potential in anticancer treatment. We would like to emphasize here that the small number of animals is one of the major limitations of the present study, and a great deal of fundamental research concerning the therapeutic effects of EMFs on cancer remains to be conducted. The most important area for study is the mechanism of the interaction between weak EMFs and living systems.

ACKNOWLEDGMENTS

We would like to thank Dr. Zhiyu Chen, Professor of the Institute of the Electronics, Chinese Academy of Sciences for his kind help in the instrumentation of EMF exporsure. This study was supported by the National Science Foundation of China (Grant No. 39770208).

REFERENCES

1. Thompson, C.B. Apoptosis in the Pathogenesis and Treatment of Disease. Science **1995**, *267*, 1456–1462.

2. Bergamaschi, G.; Rosti, V.; Danova, M.; Lucotti, C.; Cazzola, M. Apoptosis: Biology and Clinical Aspects. Haematologica **1994**, *79*, 86–93.
3. Hisamitsu, T.; Narita, K.; Kasahara, T.; Seto, A.;Yu, Y.; Asano, K. Induction of Apoptosis in Human Leukemic Cells by Magnetic Fields. Jpn. J. Physiol. **1997**, *47*, 307–310.
4. Narita, K.; Hanakawa, K.; Kasahara, T.; Hisamitsu, T.; Asano, K. Induction of Apoptotic Cell Death in Human Leukemic Cell Line, HL-60, by Extremely Low Frequency Electric Magnetic Fields: Analysis of the Possible Mechanism In Vitro. In Vivo **1997**, *11*, 329–336.
5. Ismael, S.J.; Callera, F.; Garcia, A.B.; Baffa, O.; Falcao, R.P. Increased Dexamethasone-Induced Apoptosis of Thymocytes from Mice Exposed to Long-Term Extremely Low Frequency Magnetic Fields. Bioelectromagnetics **1998**, *19*, 131–135.
6. Duke, R.C.; Cohen, J.J. Morphology and Biochemical Assays of Apoptosis. Curr. Protein Immunol. **1992**, *17* (suppl 3), 1–16.
7. Spain, J.D. *Basic Microcomputer Models in Biology*; Addison-Wesley: London, 1982; 24.
8. Repacholi, M.H. Low-Level Exposure to Radiofrequency Electromagnetic Fields: Health Effects and Research Needs. Bioelectromagnetics **1998**, *19*, 1–19.
9. Repacholi, M.H.; Greenebaum B. Interaction of Static and Extremely Low Frequency Electric and Magnetic Fields with Living Systems: Health Effects and Research Needs. Bioelectromagnetics **1999**, *20*, 133–160.
10. Blumenthal, N.C.; Ricci, J.; Breger, L.; Zychlinsky, A.; Solomon, H.; Chen, G.G.; Kuznetsov, D.; Dorfman, R. Electromagnetic Fields on Cell Attachment and Induction of Apoptosis. Bioelectromagnetics **1997**, *18* (3), 264–272.
11. Blank, M.; Goodman, R. Do Electromagnetic Fields Interact Directly with DNA? Bioelectromagnetics **1997**, *18*, 111–115.
12. Popp, F.A.; Chang J.J. Mechanism of Interaction Between Electromagnetic Fields and Living Organisms. Sci. China C Life Sci. *43*, *in press*.
13. Cadossi, R.; Hentz, V.R.; Kipp, J.; Iverson, R.; Ceccherelli, G.; Zucchini, P.; Emilia, G.; Torelli, G.; Franceschi, C. Effect of Low Frequency Low Energy Pulsing Electromagnetic Field (PEMF) on X-ray-Irradiated Mice. Exp. Hematol. **1989**, *17* (2), 88–95.
14. Cadossi, R.; Zucchini, P.; Emilia, G.; Franceschi, C.; Cossarizza, A.; Santantonio, M.; Mandolini, G.; Torelli, G. Effect of Low Frequency Low Energy Pulsing Electromagnetic Fields on Mice Injected with Cyclophosphamide. Exp. Hematol. **1991**, *19* (3), 196–201.
15. Flipo, D.; Fournier, M.; Benquet, C.; Roux, P.; Le Boulaire, C.; Pinsky, C.; LaBella, F.S.; Krzystyniak, K. Increased Apoptosis, Changes in Intracellular Ca^{2+}, and Functional Alterations in Lymphocytes and Macrophages After In Vitro Exposure to Static Magnetic Field. J. Toxicol. Environ. Health **1998**, *54* (1), 63–76.
16. Eichwald, C.; Kaiser, F. Model for External Influences on Cellular Signal Transduction Pathway Including Cytosolic Calcium Oscillations. Bioelectromagnetics **1995**, *16*, 75–85.
17. Valberg, P.A.; Kavet, R.; Rafferty, C.N. Can Low-Level 50/60 Hz Electric and Magnetic Fields Cause Biological Effects? Radiat. Res. **1997**, *148*, 2–21.
18. Reshetnyak, S.A.; Shcheglov, V.A.; Blagodatskikh, S.V. Mechanisms of Interaction of Electromagnetic Radiation with a Biosystem. Laser Phys. **1996**, *6*, 621–653.
19. Berg, H. Low-Frequency Electromagnetic Field Effects on Cell Metabolism. In

MARCEL DEKKER, INC.
270 Madison Avenue, New York, New York 10016

Bioelectrochemistry of Cells and Tissues; Walz, D., Berger, H., Eds.; Birkhauser Verlag: Basel, Boaton, Berlin, 1995; 285–301.

20. Adair, R.K. Effects of Weak High-Frequency Electromagnetic Fields on Biological Systems. In *Radio Frequency Radiation Standards: Biological Effects Edited*; Klauenberg, B.J., Grandolfo, M., Erwin, D.N., Eds.; Plenum Press: New York, 1994; 207–221.
21. Luben, R.B. Membrane Signal-Transduction Mechanisms and Biological Effects of Low-Energy Electromagnetic Fields. In *Electromagnetic Fields: Biological Interactions and Mechanism*; Blank, M., Ed.; American Chemical Society: Washington, DC, 1995; 437–450.

MARCEL DEKKER, INC.
270 Madison Avenue, New York, New York 10016